



Contents lists available at ScienceDirect

Electrochimica Acta

journal homepage: www.elsevier.com/locate/electacta



Surface oxidation of carbon supports due to potential cycling under PEM fuel cell conditions

Bharat Avasarala*, Richard Moore, Pradeep Haldar

College of Nanoscale Science and Engineering, University at Albany, SUNY, Albany, NY 12203, USA

ARTICLE INFO

Article history:

Received 11 March 2010
Accepted 21 March 2010
Available online xxx

Keywords:

Proton exchange membrane fuel cells
Catalyst support
Electrochemical oxidation
Carbon corrosion
XPS

ABSTRACT

The corrosive operating conditions of a PEM fuel cell causes significant oxidation of its carbon supports, thus severely affecting the fuel cell performance and lifetime. PEM fuel cells in transportation or automobile applications typically experience potential cycling due to start-up/shutdown cycles or varying loads further deteriorating the long-term performance of a fuel cell. Here we report that the rate of surface oxidation of carbon supports significantly increases during potential cycling making the carbon support prone to further oxidation. Using X-ray photoelectron spectroscopy, we identify the various carbon–oxygen groups formed on the surface of carbon support due to potential cycling and compare them with those treated under potential hold conditions. Interestingly, these surface groups vary in proportion from those formed on carbon support during idle potential conditions reported in the literature.

© 2010 Elsevier Ltd. All rights reserved.

1. Introduction

Fuel cells are a promising power technology with a wide variety of potential applications. With their ability to act as stationary power sources to create “micro-grids” and near-zero emissions for automobiles [1], fuel cells are being sought to solve the current energy needs and climatic problems. Particularly, proton exchange membrane fuel cells (PEM fuel cells) have received broad attention due to their low operating temperature, low emissions and quick start-up. But lifetime, reliability and cost are important factors that remain a hindrance for the wide spread commercialization of PEM fuel cells. Of these, lifetime of PEM fuel cells is considered to be the most important factor that can influence other functionality [2]. Currently, the fuel cell industry cannot match the lifetime of conventional power generation technologies, other than under the most benign and stable service conditions [3]. A significant challenge to the lifetime of a PEM fuel cell is the loss of performance during extended operation and repeated cycling [4]. Investigations have revealed that a considerable part of this performance loss is due to degradation of the electrocatalyst [5].

The carbon black supported platinum nanoparticles (Pt/C) remain the state of the art electrocatalyst for fuel cells today but they face material-limiting challenges affecting the long-term performance of a PEM fuel cell. Pt/C degradation includes the two aspects of catalyst (Pt) and one aspect of carbon support, which

influence each other. The catalytic metal, especially Pt, catalyzes the oxidation of carbon [6,7] and the oxidation of carbon further accelerates Pt sintering [8]. Vulcan XC-72 carbon black is the most popular catalyst support used currently but its durability under chemically and electrochemically oxidizing conditions needs further improvement [2].

An ideal catalyst support material should have corrosion resistance properties under strongly oxidizing conditions of PEM fuel cell: high water content, low pH (<1), high temperature (50–90 °C), high potential (>0.9 V) and high oxygen concentration. But carbon is known to undergo electrochemical oxidation to form surface oxides and CO/CO₂ under PEM fuel cell operating conditions [9–11]. Significant oxidation of carbon support can be expected to decrease the performance of a PEM fuel cell [11,12], due to the loss and/or agglomeration of Pt particles caused by the carbon corrosion. It has also been reported [12,13] that oxygen-containing groups (e.g., carboxyl, carbonyl, hydroxyl, phenol, etc.) can be formed on the carbon surface at high temperatures and/or high potentials (>1.0 V vs. RHE at room temperature or >0.8 V vs. RHE at 65 °C) which decrease the conductivity of catalysts and weaken its interaction with the support resulting in an accelerated Pt sintering [8,14,15]; thus drastically affecting the performance of PEM fuel cell.

Surface oxidation can also increase the hydrophilicity of the surface, which can result in the decrease of gas permeability [16] as the pores become more likely to be filled with liquid water that can hinder gas transport [17]. Carbon corrosion can also increase the electrode resistance by decreasing the thickness of the electrode layer [18] (as a result of carbon mass loss), which in turn decreases

* Corresponding author. Tel.: +1 518 596 8616; fax: +1 518 956 7367.
E-mail address: bavasarala@uamail.albany.edu (B. Avasarala).

the electrical contact with the current collector [19,20] of a PEM fuel cell stack.

The oxidation of carbon and the formation of surface oxides on carbon supports for long duration potential holds has been studied and the nature of C/O groups formed on carbon surface due to idle conditions has been reported [2,11]. Long idle time is a typical condition encountered by automotive PEM fuel cell stacks, i.e., the time when only idle auxiliary load power is drawn from the stack, resulting in cathode potentials of ~0.9 V and above [21].

Along with idle conditions, PEM fuel cells in automotive applications also undergo an estimated 30,000 start-up/shutdown cycles over the life of a vehicle, which can lead to short term potential excursions of the cathode electrode to 1.2–1.5 V due to H₂/air fronts in the anode compartment [22,25]. At these high potentials, corrosion rates of standard carbon supports are high, leading to large voltage degradation rates.

It has been reported [23] that fuel cells operated under cyclic conditions of the sort encountered in automotive stop-go, acceleration, and shutdown/start-up operations have a lower durability than those operated at a steady power under constant potential. Such potential cycling significantly increases carbon corrosion causing a deteriorating affect on the performance of a PEM fuel cell [23]. To the best of our knowledge, no detailed study has been conducted on the corrosion and surface oxidation of carbon black supports due to potential cycling, comparing the same under potential hold conditions of a PEM fuel cell. Through this report, we show that potential cycling can increase carbon corrosion and surface oxidation, significantly higher than the potential hold conditions.

2. Carbon oxidation

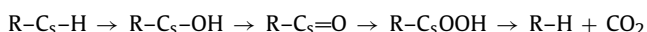
The corrosion reaction of carbon material in aqueous acid electrolytes including PEM fuel cells is generalized [24 and Refs. within] as:



This reaction is thermodynamically allowable at the potentials at which the fuel cell cathode operates [16,24], but it is believed to be slow in that potential range because of the lower temperatures of PEM fuel cells compared with phosphoric acid fuel cell. Electrochemical oxidation of carbon at room temperature to CO₂ and, to a lesser extent, CO, has been reported to increase rapidly at potentials above 0.9 V vs. RHE [24,25].

Carbon blacks, such as Vulcan XC-72, have a three-dimensional structure of microcrystalline primary particles agglomerated as amorphous clusters. Because of their heterogeneous structure and the methods used for its preparation, the primary particles exhibit a high density of surface defects. It is at these edges and corners of basal planes the carbon oxidation is initiated, since these exhibit unsaturated valences and free σ -electrons [32].

Surface oxide generation of carbon in acidic electrolytes involves the general steps of oxidation of carbon in the lattice structure followed by hydrolysis and gasification of oxidized carbon to CO₂ [24–26]. The detailed mechanism is not yet fully understood but is presumed to include parallel formation of surface and gaseous carbon oxides by disproportionate formation of oxygen functional groups [32]. One proposed generic stepwise mechanism of surface oxide formation and CO₂ evolution is shown schematically by Borup et al. [24 and Refs. within] as:



wherein the subscript 's' denotes surface species.

3. Experimental

3.1. Electrode preparation

The carbon electrode was prepared by mixing Vulcan XC-72 carbon black, IPA and Nafion solution ultrasonically and spraying the ink onto a carbon cloth (E-Tek), which is typically used in fuel cells as a gas diffusion layer. The loading of sprayed carbon black layer on the substrate was 3 mg cm⁻², with 95 wt.% of CB support and 5 wt.% of Nafion ionomer. The prepared electrode was dried at 60 °C for 10 min for any remaining solvent evaporation.

3.2. Electrochemical measurements

The electrochemical experiments were conducted in a three-electrode cell set-up where the prepared working electrode (3.0 cm × 1.0 cm) was held vertically in a chamber filled with 0.1 M HClO₄ at 60 °C. A platinum mesh and a reversible hydrogen electrode (RHE) were employed as a counter and reference electrode, respectively. All potentials are reported vs. RHE. To isolate the affects of surface oxide due to electrochemical oxidation, oxygen was removed from the solution by saturating it with argon throughout the experiment.

To simulate the start-up/shutdown cycles in an automotive PEM fuel cell stack, the working electrode was scanned potentiodynamically between 0 and 1.2 V at 50 mV s⁻¹ for 16 h or 1200 cycles, using a PARSTAT Potentiostat (Princeton Applied Research, USA). The applied potential of 1.2 V was selected in the experiments as it is common in the range of potentials encountered during start-up/shutdown operations.

For steady-state idle conditions, the potential hold experiments are performed on the electrode in a 3-electrode cell set-up at constant potentials of 0.9 and 1.2 V potentials under PEM fuel cell conditions.

3.3. X-ray photoelectron spectroscopy (XPS)

XPS analysis was performed using a ThermoFisher Theta Probe system which has a two-dimensional detector that will allow simultaneous collection of spectral data from all angles without tilting the sample. The spectrometer was equipped with a hemispherical analyzer and a monochromator and all XPS data presented in this study are acquired using Al K α X-rays (1486.6 eV) operated at 100 W. Sputter cleaning was done with a differentially pumped Ar⁺ sputter gun. The binding energies of the C 1s, O 1s, F 1s, S 2p of C electrodes were calibrated with respect to C 1s peak at 284.6 eV. Measurements were performed on the electrode samples before and after the electrochemical treatments. The sample to analyzer takeoff angle was 45°. Survey spectra were collected at pass energy (PE) of 125 eV over the binding energy range 0–1300 eV. High binding energy resolution multiplex data for the individual elements were collected at a PE of 29.55 eV. The samples for XPS characterization are dried in argon and heated at 60 °C in vacuum. The XPS spectra were background subtracted using the non-linear, Shirley method.

4. Results and discussion

4.1. Electrochemical analysis

Cyclic voltammetry (CV) is an important electrochemical characterization method that can show evidence of surface oxide formation through increased peak current assigned to the hydroquinone–quinone (HQ–Q) redox couple of carbon [11,27]. Fig. 1 shows the cyclic voltammograms (CVs) of carbon black electrode recorded during the potential cycling (0–1.2 V) at different

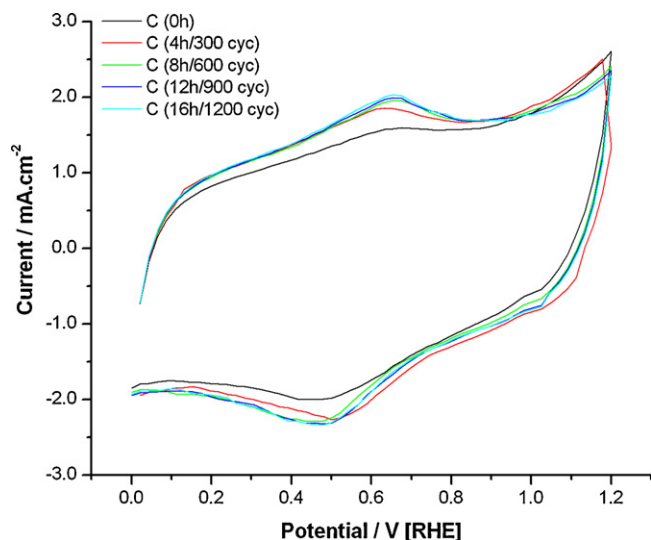


Fig. 1. Cyclic voltammogram (CV) curves of CB electrode recorded at different times during the potential cycling between 0 and 1.2 V (50 mV s^{-1}) in 0.1 M HClO_4 at 60°C for 16 h or 1200 cycles. C loading, 3 mg cm^{-2} .

times. The initial cycle of C, C (0 h) has high oxidation currents at peak potential of 1.2 V, presumably due to surface impurities which easily oxidize to CO_2 at potential $>1.0 \text{ V}$ [11]. The initial high voltammetric current peaks may also be attributed to the oxidation that started from defects on the particle surfaces. The defects are easy to corrode and upon oxidation they can further initiate the oxidation of carbon lattice.

The later cycles, C (4 h) to C (16 h), show the increase in surface oxidation currents. It is known [11] that the carbon oxidation increases rapidly above 1.0 V and hence one can see in Fig. 2 both the surface oxide peaks (at $\sim 0.6 \text{ V}$) and the oxidation peaks (at 1.2 V) due to carbon oxidation.

The steep hydroquinone–quinone (HQ–Q) peak at $\sim 0.6 \text{ V}$ for C, as shown in the anodic CV curve of Fig. 2, indicates the peak surface oxidation currents after 0, 2, 4, 8, 12 and 16 h duration. The surface charge density due to the surface reaction of the electrodes can be calculated by subtracting the pseudo-capacitance charge from total charge in the HQ–Q region [11,25] and integrating the area under

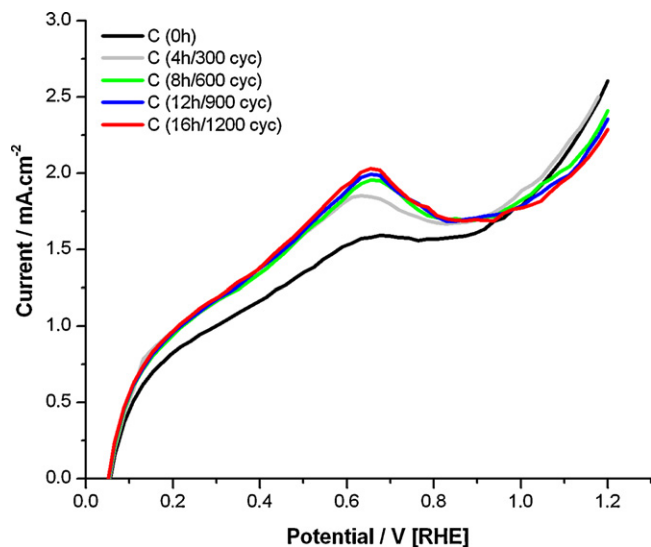


Fig. 2. Anodic CV curve of CB electrode recorded at different times during the potential cycling between 0 and 1.2 V (50 mV s^{-1}) in 0.1 M HClO_4 at 60°C for 16 h or 1200 cycles. C loading, 3 mg cm^{-2} .

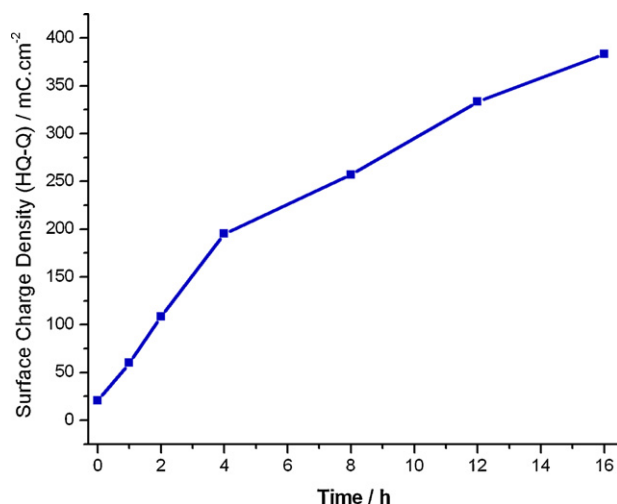
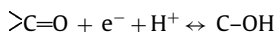


Fig. 3. The amount of the surface charge, caused due to HQ–Q redox reaction, as a function of time during the potential cycling treatment (as determined from CVs shown in Fig. 2).

the peak. This can give a representation of the amount of surface oxide (C/O) groups, formed due to potential cycling. Fig. 3 shows the surface charge density of carbon support at different times during the potential cycling in PEM fuel cell conditions. The charge thus obtained is assumed to be a faradaic charge generated from the one electron (HQ–Q) redox reaction [28–30]:



The initial surface charge density for C (0 h) in Fig. 3, is most likely due to surface contamination upon exposure to atmospheric conditions. It can be seen that the faradaic charge increases rapidly throughout the potential cycling, from an initial value of 25 to approx. 350 mC cm^{-2} after 16 h (expressed by the geometric area), which implies that the amount of HQ–Q produced on carbon black surface has increased by 14 times during potential cycling.

Considering the entire quantity of surface oxides generated following a 16 h potential cycling between 0 and 1.2 V, the electroactive HQ/Q functional groups apparently account for only a small fraction ($\sim 3\%$) of the total surface oxides generated.

4.2. Spectroscopic characterization of CB electrodes

Further evaluation of electrochemical properties was studied by spectroscopically characterizing the ‘cycled’ electrode using X-ray photoelectron spectroscopy (XPS). XPS is a surface analysis technique which can provide a better understanding of the changes on the surface due to oxidation. As carbon corrosion in low temperature fuel cells usually occurs at the surface, XPS characterization becomes a useful technique in observing the surface changes, elemental compositions, functional groups and changes in the binding energies. To study the affects of extreme conditions using XPS technique, the electrodes were evaluated under two different surface conditions: (a) and (b).

- (A) Untreated: carbon black (CB) coated electrode (as is).
- (B) Cycled: CB coated electrode after 16 h of potential cycling between 0 and 1.2 V vs. RHE at 50 mV s^{-1} in 0.1 M HClO_4 at 60°C .

To aid the analysis, XPS data cited from the literature [2,11] are used as reference. Most importantly, we did not emphasize the use of quantitative analysis to accurately identify absolute atomic % concentrations. Rather, we studied qualitative

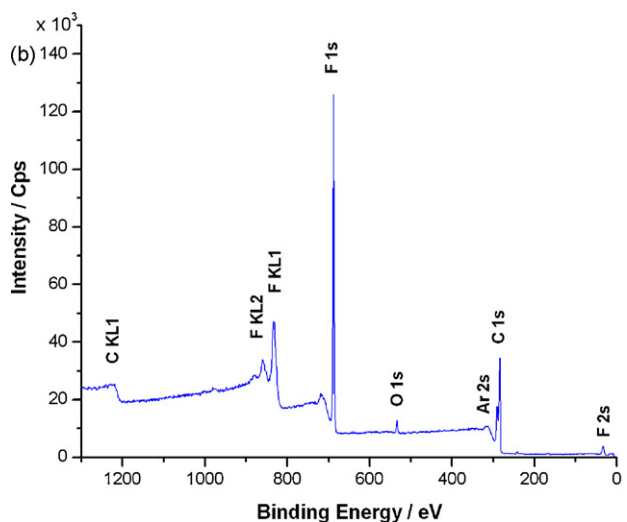
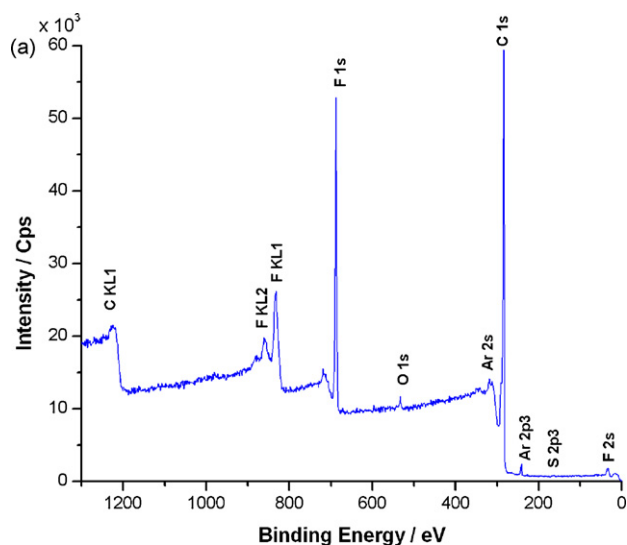


Fig. 4. XPS survey spectra of (a) untreated (b) cycled CB electrodes.

trends in the XPS data to understand the mechanisms of oxidation.

Fig. 4 shows the XPS survey scan spectra of the untreated and treated CB electrode. The signals of C, O, S and F are distinctly detected on the 'untreated' electrode. As anticipated, the F and C peaks can be seen as dominating, attributed to the perfluorinated Nafion ionomer and carbon black, respectively. After the potential cycling treatment, the F peak dominates while the C peak decreases significantly.

The trends of the surface atomic percentage concentrations (at.% conc.) of these elements are determined from the XPS intensities considering their sensitivity factors and the trends are presented in Fig. 5. The atomic concentration of C dropped significantly, by ~20% at.% conc. after potential cycling. The decrease of C is not followed by a corresponding increase in the oxygen concentration by the same amount, which can mean that carbon oxidation process did not take place via the 'surface oxides' but was predominantly through the 'gaseous oxides'. This suggests that the decrease of carbon is due to the electrochemical oxidation of C to CO/CO₂ that can specifically result in a mass loss of the electrode.

Table 1 shows the O/C atomic ratio obtained from the XPS analysis of the O and C peaks of Fig. 4(a) and (b). O/C ratio increases from 0.01 to 0.04, which indicates towards the significant decrease in carbon composition over oxygen. This further suggests that car-

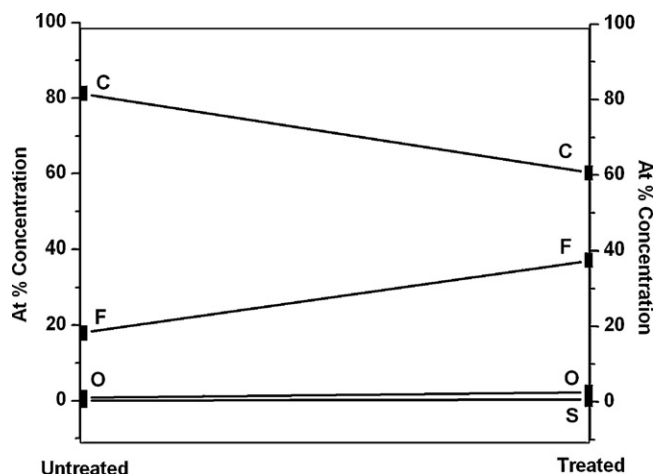


Fig. 5. Relative atomic % concentrations of surface elements on untreated and cycled CB electrodes obtained using XPS survey spectra.

bon prefers forming gaseous oxides over surface functional groups during potential cycling. It also indicates that the oxidation degree of carbon black [2,31] increases with potential cycling.

The initial composition of oxygen on the untreated CB electrode can be attributed mainly to the surface impurities formed due to the exposure of carbon black to atmospheric conditions. This composition is bound to vary and depends, largely, on the storage and/or pre-treatment conditions of the carbon support. Though the overall oxygen composition in this case is relatively small for the 'cycled' CB electrode, it is on an increasing trend due to potential cycling. Since oxygen is a representation of the various carbon–oxygen (C/O) functional groups formed on the carbon support surface, its increase suggests the increase in surface oxidation. It is reported that the electroactive HQ–Q functional groups usually account for only a small fraction of the total surface oxygen generated during electrochemical oxidation of carbon [11]. The surface charges in this case, calculated from the CV curve in Fig. 2 by the formula: area (HQ–Q)/area (anodic curve), contribute 3.4% of the total current density for the 'cycled' electrode after 16 h duration.

A comparison of the surface properties of the 'untreated' and 'cycled' CB electrodes is made so far and it is concluded that potential cycling significantly increases the carbon corrosion and leads to the formation of various C/O functional groups. The identification of the different functional groups was carried out by deconvolution of the C 1s XPS peaks for the untreated and cycled CB electrodes and presented in Fig. 6(a) and (b), respectively. The deconvoluted C 1s XPS spectra provides evidence for the presence of several surface oxide functionalities namely, carboxyl/lactones, ether/hydroxyl, and ketones [2,11], and the most probable assignments to the origin of these functionalities are presented in Table 2.

It is also our hypothesis that potential cycling has a higher impact on the electrochemical oxidation of carbon support than the potential hold conditions operated in a fuel cell. To validate this, two CB electrodes are electrochemically treated under constant potentials of 0.9 and 1.2 V, respectively, for a period of 16 h. For a useful one-to-one comparison, the potential hold experiments

Table 1

The atomic ratios of carbon and oxygen elements on the surface of CB electrodes – untreated and cycled, obtained from the atomic concentrations of XPS survey spectra in Fig. 4.

CB electrode	Ratio O/C
Untreated	0.01
Cycled	0.04

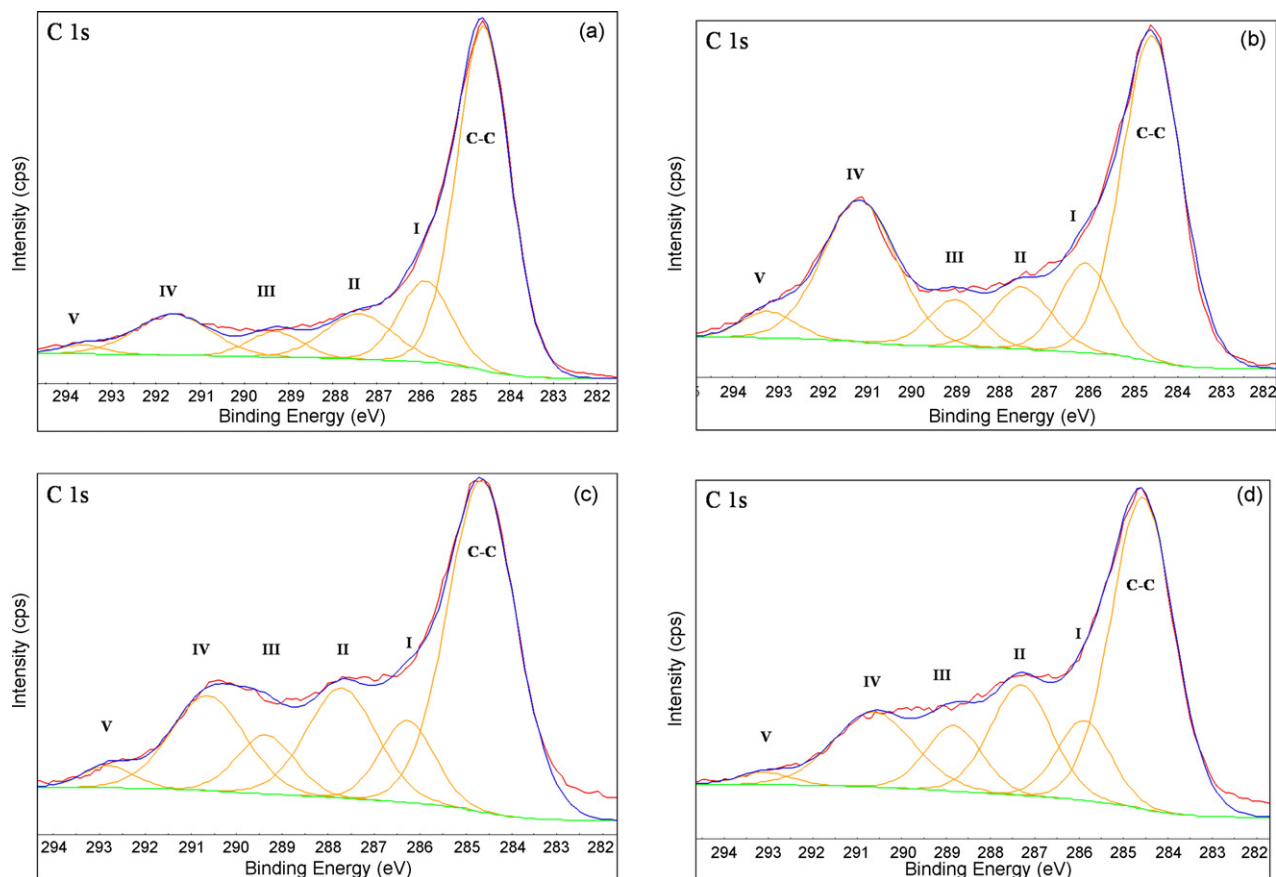


Fig. 6. Deconvoluted C 1s high resolution XPS spectra of CB electrodes: (a) untreated, (b) cycled, (c) ‘0.9V potential hold’ treated and (d) ‘1.2V potential hold’ treated.

were also conducted under identical PEM fuel cell conditions used for ‘potential cycling’ treatment. The ‘0.9V potential hold’ and ‘1.2V potential hold’ treated electrodes were spectroscopically analyzed using XPS techniques and the various functional groups derived through deconvolution of their C 1s XPS peaks are presented in Fig. 6(c) and (d), respectively.

One can see the distribution of the various (C/O) functional groups due to the different electrochemical treatments in the deconvoluted peaks of C 1s in Fig. 6. The approximate contributions of the functional groups to the overall C 1s signals for the ‘treated’ CB electrodes are presented in Table 3. There is a significant difference in the distribution of the above (O/C) functional groups on the surface of carbon supports treated differently. Of the surface (C/O) groups on ‘cycled’ CB electrode, C–O has a dominant presence compared to C=O and C–OO while the C=O functional groups take the predominance over the C–O and C–OO groups for the ‘potential hold’ treatment CB supports. Kangasniemi et al. [11] reported a similar decrease of C–O groups and an increase in C=O functional groups for carbon black electrode after a potential hold of 1.2V for 120 h.

Table 2
Assignments of the deconvoluted peaks of the high resolution C 1s XPS spectra.

Functional groups C 1s	Binding energy (eV)	Assignment
C–C	284.6	C–C bonding
I	286.1	C–O
II	287.6	C=O
III	288.4	C–OO
IV	290.6	C–F
V	292.8	C–H–F

Fig. 7 compares the amount of oxygen formed on the surface of carbon supports due to electrochemical oxidation of the CB electrodes exposed to potential cycling (0–1.2V) and potential hold (0.9 and 1.2V) treatments. From earlier discussion, it is known that carbon corrosion increases at potentials >0.9V while C/O functional groups (surface oxides) are prone to form at lower potentials [11]. In such a case, the gain in C/O groups should be lower for a CB electrode exposed to ‘1.2V potential hold’ treatment while the sur-

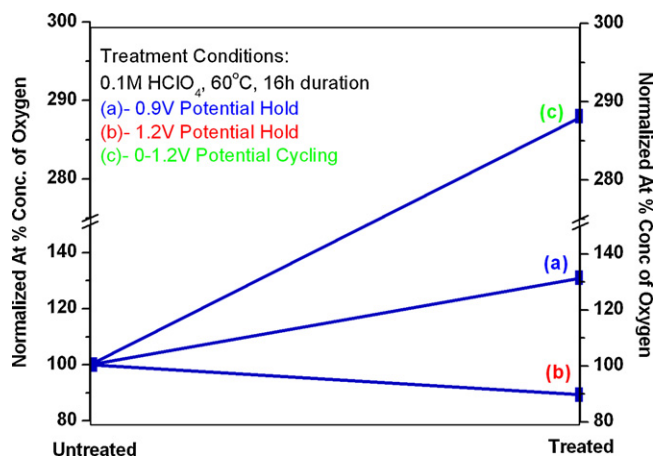


Fig. 7. A normalized comparison of the oxygen composition on the surface of carbon supports after treatments under the following conditions: (a) potential hold at 0.9V (b) potential hold at 1.2V and (c) potential cycling between 0 and 1.2V at 50 mV s⁻¹. All tests are conducted in 0.1 M perchloric acid saturated with argon and at 60 °C. The oxygen compositions are derived from the XPS survey spectra of the respective CB electrodes after the electrochemical treatment.

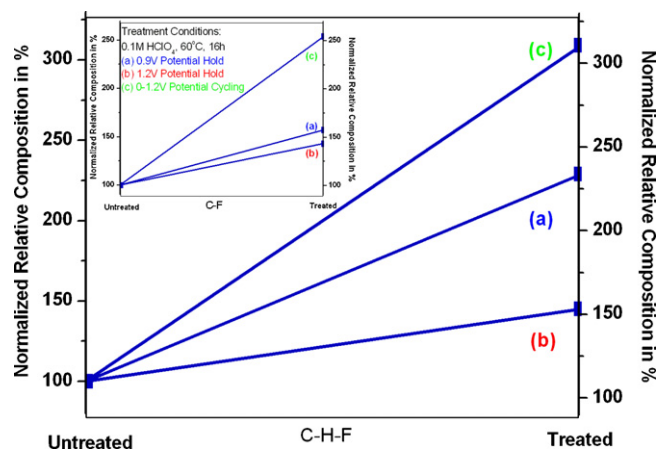


Fig. 8. A normalized comparison of the C–H–F and C–F (inset) groups on the surface of carbon supports after treatments. The treatment conditions and the trend assignments remain the same as in Fig. 7.

face oxygen groups should be higher for the CB electrode exposed to 0.9 V potential hold. This can be seen in Fig. 7, where the relative composition of oxygen has decreased for '1.2 V potential hold' treated electrode while the same has increased for '0.9 V potential hold' treated CB electrode.

Compared to the two potential hold treatments, the 'cycled' CB electrode shows the maximum gain of oxygen with a greatest increase in the C/O functional groups on its surface making the support prone to further corrosion. This agrees to our earlier electrochemical analysis where the starting operating potential is seen (Fig. 2) to decrease, making the carbon support prone to corrosion at earlier potentials upon prolonged exposure to potential cycling. The increased presence of carbon/oxygen functional groups rapidly oxidize to gaseous oxides, corroding the surface and thus resulting in carbon mass loss.

4.3. Nafion ionomer degradation

During the XPS analysis, an unusually high presence of fluorine is observed for the treated CB electrodes as can be seen in the XPS survey in Fig. 4. The atomic concentration of F is also seen to be on an increasing trend, in Fig. 5, after the potential cycling. An increase of the C–F and C–H–F functional groups in C 1s of Fig. 6 can also be seen for the 'treated' CB electrodes exposed to potential cycling and potential hold treatments. The increase in composition can be mainly attributed to the degradation of Nafion[®] ionomer, i.e., its (C–F)_n polymer chain and its SO₃ side groups. It can also be possible that the fluorine composition increases when the ionomer, seeped into the pores of the carbon supports, is released to the surface during the electrochemical treatment and is characterized by the XPS beam as a newly formed functional group. The occurrence of this phenomenon is not disagreed and is the reason for an increase in F 1s signal in the XPS survey but such a case would result in an evenly distributed increase of all functional groups associated with fluorine. Along with an overall increase of the fluorine peaks in C 1s, Fig. 6 shows the significant increase of the (C–F) functional group and the strong presence of a hitherto negligible (C–H–F) functional group on the 'cycled' electrode. While the increase in C–F functional group can be attributed to the breaking of its long (C–F)_n polymer chains, the increase of C–H–F functional group is most likely due to the reaction of C–F groups with the hydrogen compounds.

The trends of the relative compositions of C–F and C–H–F groups (of C 1s) from the treated and untreated CB electrodes are plotted in Fig. 8. Though both the potential hold treatments caused similar trends of increase in C–F and C–H–F functional groups, these trends

Table 3

Approximate functional group distribution in C 1s observed by XPS for 'untreated' and 'treated' CB electrodes (excluding the CC, CF and CHF groups).

Functional groups	Deconvoluted peaks relative distribution (%)		
	Potential cycling	0.9 V potential hold	1.2 V potential hold
C–O	47	24	21
C=O	31	62	52
C–OO	22	20	27
Total	100	100	100

were seen to be more prominent in '0.9 V potential hold' case indicating that 0.9 V significantly affects the Nafion[®] ionomer than the higher potentials of 1.2 V. Fig. 8 also shows that potential cycling affects Nafion[®] ionomer the most, when compared to the potential hold treatments. As can be seen, the affects on the C–F and C–H–F functionalities of CB supports are significantly more severe compared to the affects caused by potential hold treatments. Though the phenomenon and its explanation is beyond the scope of this report, such degradation of Nafion ionomer will have obvious negative affects on the membrane durability and thus on the long-term performance of a PEM fuel cell.

It is known that the carbon corrosion is initiated at the defects on the particle surface, the generation of which is significantly dependent on the manufacturing methods of carbon black. Hence, it is emphasized that the surface groups formation and distribution on carbon black support are specific to the conditions and material (Vulcan XC-72) used in this report.

5. Conclusion

From the above results derived from XPS and CV analysis, it can be concluded that the carbon oxidizes substantially upon potential cycling, through surface oxidation resulting in formation of surface C/O compounds and direct oxidation to CO₂ and/or CO. The C 1s peaks from XPS, the CV behavior of carbon and the ratios of carbon functional groups after electrochemical treatment match well with the reported literature [12 and Refs. within]. It is shown [11] that potentially holding carbon black in PEM fuel cell conditions results in the formation of surface (C/O) groups of similar proportion, and match well with the reported literature. During potential cycling, the dominant surface group is reported as C–O functional group.

In summary, we have investigated the electrochemical oxidation of carbon black due to potential cycling between 0 and 1.2 V in 0.1 M perchloric acid at 60 °C, which mimics the extreme working condition of proton exchange membrane fuel cells. It is found that several oxygen-containing functional groups such as C=O, C–O–C, O–C=O are formed on carbon black when a cyclic potential between 0 and 1.2 V is applied for 16 h duration. The increase in HQ–Q and total surface oxygen on the surface of carbon black during potential cycling is much higher compared to as-received carbon black. It can be concluded that, under the conditions used in this work, potential cycling significantly increases the surface oxidation along with significant oxidation to gaseous oxides such as CO/CO₂ gases. The oxygen functional groups formed on the surface of the potentially cycled CB supports were found to be relatively higher compared to those exposed to 'potential hold' conditions.

References

- [1] B. Avasarala, P. Haldar, J. Power Sources 188 (2009) 225.
- [2] Y. Shao, G. Yin, Y. Gao, J. Power Sources 171 (2007) 558.
- [3] G. Hinds, NPL Report DEPC–MPE 002, September 2004.
- [4] H. Gasteiger, W. Gu, R. Makharia, M.F. Mathias, B. Sompalli, in: W. Vielstich, H. Gasteiger, A. Lamm (Eds.), Fuel Cell Technology and Applications, Beginning-of-life MEA Performance-efficiency Loss Contributions, Handbook of Fuel Cells – Fundamentals, Technology and Applications, vol. 3, John Wiley & Sons Ltd., 2003 (Chapter 46).

- [5] T. Tada, T. Kikinzoku, in: W. Vielstich, H. Gasteiger, A. Lamm (Eds.), *Fuel Cell Technology and Applications, Handbook of Fuel Cells – Fundamentals, Technology and Applications*, vol. 3, John Wiley & Sons Ltd., 2003.
- [6] Z. Siroma, K. Ishii, K. Yasuda, Y. Miyazaki, M. Inaba, A. Tasaka, *Electrochem. Commun.* 7 (2005) 1153.
- [7] L. Li, Y.C. Xing, *J. Electrochem. Soc.* 153 (2006) A1823.
- [8] Y.Y. Shao, G.P. Yin, Y.Z. Gao, P.F. Shi, *J. Electrochem. Soc.* 153 (2006) A1093.
- [9] K. Kinoshita, *Carbon: Electrochemical and Physicochemical Properties*, Wiley, New York, 1988.
- [10] J. Willsau, J. Heitbaum, *J. Electroanal. Chem.* 161 (1984) 93.
- [11] K.H. Kangasniemi, D.A. Condit, T.D. Jarvi, *J. Electrochem. Soc.* 151 (2004) E125.
- [12] S.D. Knights, K.M. Colbow, J. St-Pierre, D.P. Wilkinson, *J. Power Sources* 127 (2004) 127.
- [13] L.M. Roen, C.H. Paik, T.D. Jarvic, *Electrochem. Solid-State Lett.* 7 (2004) A19.
- [14] Y.Y. Shao, G.P. Yin, J. Zhang, Y.Z. Gao, *Electrochim. Acta* 51 (2006) 5853.
- [15] F. Coloma, A. Sepulvedaescrignano, F. Rodriguezreinoso, *J. Catal.* 154 (1995) 299.
- [16] Z. Siroma, N. Fujiwara, T. Ioroi, S. Yamazaki, K. Yasuda, Y. Miyazaki, *J. Power Sources* 126 (2004) 41.
- [17] M. Fowler, J.C. Amphlett, R.F. Mann, B.A. Peppley, P.R. Roberge, *J. New Mater. Electrochem. Syst.* 5 (2002) 255.
- [18] E. Guilminot, A. Corcella, F. Charlot, F. Maillard, M. Chatenet, *J. Electrochem. Soc.* 154 (2007) B96.
- [19] C. He, S. Desai, G. Brown, S. Bollepalli, *Interface* 14 (2005) 41.
- [20] M.K. Debe, A. Schmoeckel, S. Hendricks, G. Vernstrom, G. Haugen, R. Atanasoski, *ECS Trans.* 1 (2006) 51.
- [21] B. Du, Q. Guo, R. Pollard, D. Rodriguez, C. Smith, J. Elter, J. Miner, *Met. Mater. Soc.* 58 (2006) 45.
- [22] C.A. Reiser, L. Bregoli, T.W. Patterson, J.S. Yi, J.D.L. Yang, M.L. Perry, T.D. Jarvi, *Electrochem. Solid-State Lett.* 8 (2005) A273.
- [23] B. Merzougua, S. Swathirajan, *J. Electrochem. Soc.* 153 (12) (2006) A2220.
- [24] S. Borup, et al., *Chem. Rev.* 107 (10) (2007) 3904.
- [25] M.F. Mathias, R. Makharia, H.A. Gasteiger, J.J. Conley, T.J. Fuller, C.J. Gittleman, S.S. Kocha, D.P. Miller, C.K. Mittelsteadt, T. Xie, S.G. Yan, P.T. Yu, *Electrochem. Soc. Interface* 14 (2005) 24.
- [26] M. Cai, M.S. Ruthkosky, B. Merzougui, S. Swathirajan, M.P. Balogh, S.H. Oh, *J. Power Sources* 160 (2006) 977.
- [27] E. Passalacqua, P.L. Antonucci, M. Vivaldi, A. Patti, V. Antonucci, N. Giordano, K. Kinoshita, *Electrochim. Acta* 37 (1997) 2725.
- [28] J.H. Chen, W.Z. Li, D.Z. Wang, S.X. Yang, J.G. Wen, Z.F. Ren, *Carbon* 40 (2002) 1193.
- [29] J.S. Ye, X. Liu, H.F. Cui, W.D. Zhang, F.S. Sheu, T.M. Lim, *Electrochem. Commun.* 7 (2005) 249.
- [30] P.N. Ross Jr., J. Lipkowski, P.N. Ross (Eds.), *Electrocatalysis*, Wiley-VCH, New York, 1998, p. 54.
- [31] J.L. Figueiredo, M.F.R. Pereira, M.M.A. Freitas, J.J.M. Orfao, *Carbon* 37 (1999) 1379.
- [32] S. Maass, F. Finsterwalder, G. Frank, R. Hartmann, C. Merten, *J. Power Sources* 176 (2008) 444.